Theory of fast time evolution of nonequilibrium spin states in magnetic heterostructures

I. A. Yastremsky,[1] Peter M. Oppeneer,[2] and B. A. Ivanov[1,3,*]
[1]*Taras Shevchenko National University of Kiev, 03127 Kiev, Ukraine*
[2]*Department of Physics and Astronomy, Uppsala University, P. O. Box 516, SE-75120 Uppsala, Sweden*
[3]*Institute of Magnetism, National Academy of Sciences of Ukraine, 03142 Kiev, Ukraine*
(Received 10 May 2014; revised manuscript received 7 June 2014; published 16 July 2014)

The temporal evolution of highly nonequilibrium and spatially nonuniform spin states is analyzed on the basis of a general, phenomenological spin dynamics theory, employing the concept of both local (relativistic) and nonlocal (exchange) spin relaxations. The developed theory is applied here to describe the ultrafast spin evolution arising after the action of a femtosecond laser pulse on magnetic heterostructures containing layers of two different ferromagnets; specifically, we consider here both Ni-Fe and Ni-Ru-Fe heterostructures. As a consequence of the laser excitation, nonuniform spin distributions are created in the layered systems, which form the initial state for the spin dynamics calculations. The results obtained provide an explanation of recent experiments on the magnetization recovery in laser-pumped Ni-Ru-Fe heterostructures. The importance of the nonlocal character of the magnetization recovery for such systems is established. In particular, the experimentally observed strong dependence of the spin recovery on the relative orientation of the magnetic moments of the layers is explained theoretically. If the nonlocal spin relaxation is dominating, the evolution from an initial nonuniform magnetization profile is concurrent with the creation of a strong spin current flowing between the layers.

DOI: 10.1103/PhysRevB.90.024409 PACS number(s): 75.78.Jp, 75.75.−c, 75.10.Hk

I. INTRODUCTION

The excitation of magnetic materials with short laser pulses has revealed fascinating and unexpected magnetization dynamics. An unanticipated, fast laser-induced demagnetization within a few hundred femtoseconds was observed in elemental 3*d* ferromagnets such as nickel [1–4]. As the demagnetization time is much shorter than the characteristic magnetization evolution time, this discovery has initiated intensive research in ultrafast laser-induced magnetization dynamics (see, e.g., Ref. [5]) and has led to a fierce debate as to what mechanisms could be responsible for the ultrafast demagnetization [6–15].

Even though the mechanisms of laser-induced demagnetization in elemental ferromagnets are not yet unambiguously clarified, recent experimental efforts have focused on laser-induced magnetization dynamics in *inhomogeneous* magnetic materials [16–21]. Several different kinds of inhomogeneous materials have recently been studied. Magnetic alloys containing more than one sublattice with distinct sublattice magnetizations, such as ferromagnetic FeNi alloy [17] and ferrimagnetic GdFeCo alloy [16], revealed recently unusual spin dynamics, connected to the different exchange-coupled spin angular moments present on the sublattices. The excitation of GdFeCo alloys with a short laser pulse caused a switching of the magnetization on a picosecond time scale [16], something which holds promise for the development of ultrafast magnetic recording. The origin of the switching is in the focus of recent theoretical studies [22–24]. Other inhomogeneous materials which were recently investigated are various rare-earth–transition-metal alloys (TbCo, GdCo) [21] and thin magnetic films with magnetic inhomogeneities (domains) and/or chemical inhomogeneity [18–20]. An ultrafast spin angular momentum transfer between different lateral regions in the magnetic films has been observed in the latter studies, as well as between the different sublattices in the investigation of the alloys [21].

A third class of recently investigated inhomogeneous materials—which is the focus of the present study—is that of layered metallic heterostructures [25–27], as well as layered magnetic tunnel junctions [28], for which laser-induced switching is a recent goal [29,30]. Laser excitation of a Ni-Ru-Fe trilayer system from the Ni side revealed an intriguing, entangled spin dynamics in the interlayer exchange coupled Ni and Fe layers: for a parallel alignment of the Ni and Fe magnetizations, demagnetization of the Ni layer led to an ultrafast magnetization increase of the Fe layer, whereas for an antiparallel alignment of the Ni and Fe magnetizations, demagnetization of the Ni layer caused a demagnetization of the Fe layer [25]. The unusual spin response measured on the Fe layer has been explained by a superdiffusive spin current perpendicular to the layers, causing an ultrafast spin transfer from the Ni to the Fe layer [25]. This initial spin transfer, due to superdiffusive nonequilibrium, nonthermal carriers [13,31], is expected to be active until electron thermalization has occurred, which for metals happens approximately in some 300 femtoseconds [32–34]. After electron thermalization, a further unusual spin evolution has been observed [25,35]: the spin relaxation back to equilibrium is much faster for the antiparallel configuration of the Ni and Fe magnetizations than for the parallel configuration.

The difference in spin evolution of the two configurations is intriguing. The Ruderman-Kittel-Kasuya-Yoshida (RKKY) coupling between the layers is typically very weak, so that in the first instance no difference would be expected for the spin evolution in the two layers treated, say, on the basis of the Landau-Lifshitz (LL) equation [36] or the Landau-Lifshitz-Bloch (LLB) equation [37], which are both local, and spin dynamics would hence proceed independently in the two layers, and even in different points of the system

*bivanov@i.com.ua

(see the discussion in Sec. III A). This suggests that a different theoretical formulation needs to be developed to explain the observed spin evolutions.

Here we develop such a formulation, which, in contrast to the Landau-Lifshitz model, builds on *longitudinal* spin dynamics. The following ideas were used for deriving a qualitative description of the experimental observations. The laser pulse (with duration of less than 100 fs) has, after electron thermalization, induced a highly nonequilibrium magnetization distribution, which plays the role of an initial condition for the subsequent magnetization dynamics, which are described by an equation for longitudinal spin dynamics derived from Bar'yakhtar's equation [38–40], called also LLBar equations [41]. The time evolution of the initial state at times longer than 0.5 ps can appropriately be evaluated with evolution equations for the individual layer magnetizations alone, in a manner similar to a recent treatment of sublattice magnetization dynamics [23]. Our analysis of the longitudinal spin dynamics reveals the conditions under which the rate of the spin recovery back to equilibrium depends strongly on the configuration of layer magnetizations, that is, whether these are antiparallel or parallel. The here-developed theory is anticipated to be important for predicting fast magnetization equilibration and possibly reversal in coupled magnetic layered systems.

II. MODEL

A. Theoretical formulation

The Landau-Lifshitz equation [36], with the standard relaxation terms [36,42], preserves the magnetization length. This fact limits the applicability of the LL equation to the dynamics of the unit vector of the normalized magnetization, a restriction which was already mentioned in the original article [36]. Note that the commonly used relaxation terms [36,42] give in fact equivalent expressions.

The question of what the correct structure of the relaxation terms in the LL equation should be was previously considered by Bar'yakhtar [38–40]. On the basis of general symmetry arguments and Onsager relations, Bar'yakhtar derived the general form of such an equation for the magnetization dynamics, which comprises two distinct relaxation terms, one of relativistic origin and a nonlocal spin-conserving relaxation term, giving a purely exchange related relaxation. The resulting expression can be written as [38]

$$\frac{\partial \vec{M}}{\partial t} = -\gamma[\vec{M}\times\vec{H}_{\rm eff}] + \lambda_{\rm r}\vec{H}_{\rm eff} - a^2\lambda_{\rm nl}\nabla^2\vec{H}_{\rm eff}, \qquad (1)$$

where γ is the gyromagnetic ratio, $\lambda_{\rm r}$ is a relativistic relaxation constant, $\lambda_{\rm nl}$ is a nonlocal (exchange) relaxation constant, $\vec{H}_{\rm eff} = -\delta\Phi/\delta\vec{M}$ is an effective magnetic field, and Φ is a thermodynamic potential. The multiplier a^2 (a is of the order of the lattice constant) is added to have the same dimension for both damping constants, $\lambda_{\rm r}$ and $\lambda_{\rm nl}$. It is worth noting here that not only is the nonlocal term with $\lambda_{\rm nl}$ in Eq. (1) absent in the standard equations, but also the form of the relativistic term differs from that of the standard relaxation terms, which are, as mentioned, limited to the dynamics of the normalized magnetization.

To illustrate the differences between the standard formulation and that of Bar'yakhtar, we note that the Eq. (1) describes both the standard (transversal) LL dynamics of the magnetization of a ferromagnet corresponding to the magnetization precession around the effective field, as well as the longitudinal dynamics. To clarify this, let us assume $\vec{M} = M\vec{m}$, $\vec{m}^2 = 1$ and rewrite Eq. (1) as the set of equations for the unit vector $\vec{m}$ and the modulus M,

$$\frac{\partial \vec{m}}{\partial t} = -\gamma[\vec{m}\times\vec{H}_{\rm eff}] + \frac{\lambda_{\rm r}}{M}[\vec{H}_{\rm eff} - \vec{m}(\vec{m}\cdot\vec{H}_{\rm eff})] + a^2\lambda_{\rm nl}[\vec{m}(\vec{m}\cdot\nabla^2\vec{H}_{\rm eff}) - \nabla^2\vec{H}_{\rm eff}], \qquad (2)$$

$$\frac{\partial M}{\partial t} = \lambda_{\rm r}(\vec{m}\cdot\vec{H}_{\rm eff}) - \lambda_{\rm nl}a^2(\vec{m}\cdot\nabla^2\vec{H}_{\rm eff}), \qquad (3)$$

where $(\vec{m}\cdot\vec{H}_{\rm eff}) = -\delta\Phi/\delta M$.

Note first that the equation for the transversal variable $\vec{m}$ with $\lambda_{\rm nl} = 0$ has the form of the LL equation, and the relativistic relaxation term in the equation adopts the standard Landau-Lifshitz form. It is equivalent to the commonly used Gilbert damping term with the dimensionless Gilbert damping constant $\alpha_G = \lambda_{\rm r}/\gamma M$ at small α_G. The transversal dynamics and relaxation differ from the standard one only by the presence of a specific nonlocal exchange contribution with $\nabla^2\vec{H}_{\rm eff}$. This term is of significant importance, because it determines the correct asymptotic form of the magnon damping γ_k at large wave vector $k \to \infty$, which is of the form $\gamma_k \propto \lambda_{\rm nl}\omega_k k^2$, where the magnon frequency $\omega_k \propto k^2$; see Ref. [38]. This asymptotic behavior is in accordance with the well-known result of the microscopic theory by Dyson [43].

The transversal dynamics is characterized by the relatively long precession time $2\pi/\gamma H_{\rm eff}^{\perp}$, where $H_{\rm eff}^{\perp} = |\vec{H}_{\rm eff}^{\perp}|$, $\vec{H}_{\rm eff}^{\perp}$ is the transversal (with respect to the magnetization $\vec{M}$) part of the effective field. $H_{\rm eff}^{\perp}$ originates from several magnetic interactions (Zeeman energy, magnetic anisotropy, demagnetizing field) and it rarely exceeds 1 T. Thus, the characteristic time of the transversal dynamics is of the order of nanoseconds, much longer than the subpicosecond exchange time.

Evidently, Eq. (1) (even for $\lambda_{\rm nl} = 0$) describes a much faster spin dynamics regime, corresponding to the change of *the modulus of magnetization*. If only the relativistic term in Eq. (1) is taken into account, the equation for M adopts the form of the Landau-Khalatnikov equation [44], $\partial M/\partial t = -\lambda_{\rm r}\delta\Phi/\delta M$. This equation was originally used for the description of the evolution of the modulus of the order parameter of He II, and it is well confirmed by experiments. For ferromagnets, this equation describes the uniform relaxation of the magnetization modulus M to its equilibrium value M_0, in the linear approximation $M - M_0 \propto \exp(-t/t_0)$, with the relaxation rate $1/t_0$ being of relativistic origin, but exchange enhanced [38]. The value of t_0 found from Eq. (1) is of the order of picoseconds in accordance with the microscopic theory, based on the nonequilibrium thermodynamics of the magnon gas [45].

The equation for $\vec{M}$, containing a relaxation term of the form of $\hat{\lambda}\vec{H}_{\rm eff}$, with the coefficient $\hat{\lambda}$ anisotropic with respect to $\vec{m}$, is known as the Landau-Lifshitz-Bloch equation; it is frequently considered as a good approximation for nonsmall

temperatures [37,46], as was confirmed by atomistic spin dynamics simulations [47]. It is worth to note here that the anisotropy of the tensor $\hat{\lambda}$ plays no role for the case of our interest, the fast longitudinal magnetization dynamics.

The two completely different spin dynamics regimes, longitudinal and transversal, are thus both described by Eq. (1) and are governed by two universal relaxation constants, λ_r and λ_{nl}. This offers the possibility to determine these constants from different experiments. For example, the value of λ_r (or, equivalently, Gilbert constant α_G) found, say, from ferromagnetic resonance measurements, can be then used for the analysis of uniform perturbations of M. The exchange constant λ_{nl} can be determined from the aforementioned asymptotic behavior for short-wave magnon damping, and then used for description of highly nonuniform evolution of M. In particular, the value of λ_{nl} was estimated for magnetic dielectrics like yttrium-iron garnet [38]. For itinerant-electron ferromagnets, the short-wavelength asymptotics for magnons decrement (called q^2 damping) was recently calculated microscopically [48] and gives a temperature-independent λ_{nl}.

In the linear approximation the two equations, (2) and (3), are uncoupled. The coupling of M with $\vec{m}$ gives an additional channel of dissipations for nonlinear excitations, like magnetic domain walls [49], solitons [50], and Bloch points [51]. For all the above problems—occurring on a comparably long time scale—the quantity $M - M_0$ can be considered as a slave variable; it follows the dynamics of $\vec{m}$ with the same characteristic time as for transversal dynamics.

In contrast, for the problem of ultrafast magnetization dynamics in ferromagnets, the initial state contains nonsmall longitudinal deviations of the magnetization from the equilibrium. Thus, in the evolution of these states the longitudinal dynamics dominates; the characteristic time is of the order of t_0 and it is *faster* than that for standard transversal dynamics. The transversal deviations of $\vec{M}$, even if they are present in the initial state, just cannot develop during such a short time [52]. Thus, the longitudinal dynamics can be treated independently, a fact that will be used in the analysis below.

The analysis will be done with full accounting of both constants, λ_{nl} and λ_r, which act completely differently. As we have mentioned above, when neglecting λ_{nl}, the equation for M acquires the form of a nonlinear diffusion equation (NDE) with a nonlinear source term, i.e., $\partial M/\partial t = \lambda_r A \nabla^2 M - \lambda_r \partial \Phi_{un}/\partial M$. Here Φ_{un} is the part of Φ, not containing the gradients of M and leading to nonconservation of the total spin of the system, A is a nonuniform exchange constant [see below Eq. (5)].

Such NDE was first studied in the pioneering works by Kolmogorov, Petrovsky, and Piskounov [55] and by Fisher [56] to treat propagations of some nonlinear wave (diffusive front) into the region occupied by the unstable state. In magnetism the NDE was used for a description of moving domain walls and solitons in weak ferromagnets [57] and processes of formation of longitudinal waves after the ultrafast demagnetization in ferromagnets [58].

In the opposite case, with negligible λ_r, the character of the evolution is completely different. It is clear that the exchange interaction cannot change the total spin of the system, and the pure exchange evolution of the magnetization for a simple ferromagnet is described by an equation of the form of a local conservation law [38], $\partial \vec{M}/\partial t = -\partial \vec{j}_i^{(M)}/\partial x_i$, where $\vec{j}_i^{(M)}$ is the spin current; see further below for the concrete form of this equation. If both the relaxation channels are accounted for, i.e., $\lambda_{nl} \neq 0$ and $\lambda_r \neq 0$, the equation for M is much more complicated; it contains nonlinear terms with $\nabla^2 M$ as well as the term with $\nabla^4 M$. Most of the rigorous mathematical methods, developed for the NDE, cannot be extended to higher-order equations [59,60]. Thus, one can expect that the character of the magnetization evolution depends strongly on the ratio of these two constants. In this respect, it is essential that longitudinal spin evolutions of different kinds arise naturally within the relatively simple equation (3), even within the approximation of purely longitudinal dynamics. Our analysis will be done with full accounting for both constants, λ_{nl} and λ_r, which act completely differently.

B. Modeling the heterostructures

Considering now the typical sample geometry of the recent experiments to probe the ultrafast spin dynamics in Ni-Fe and Ni-Ru-Fe heterostructures [25,26], we note that the size of the focused light spot is much larger than the thickness of each layer and of the whole structure. The initial spin deviation strongly depends on the coordinate x, chosen here perpendicular to the structure, but within the spot region it is practically uniform in the plane of the structure. Thus, a quasi-one-dimensional evolution with $M = M(x,t)$ is expected for our problem. As has been mentioned in the above section, we can limit ourselves to the *longitudinal* dynamics only, and Eq. (3) for the length of the magnetic moment $M = |\vec{M}|$ acquires the form

$$\frac{\partial M}{\partial t} = \lambda_r H_{\text{eff}} - a^2 \lambda_{nl} \frac{\partial^2 H_{\text{eff}}}{\partial x^2}. \tag{4}$$

For the thermodynamic potential we adopt the Landau model

$$\Phi = \frac{1}{8\chi_\parallel M_0^2}\left(M^2 - M_0^2\right)^2 + \frac{A}{2}\left(\frac{\partial M}{\partial x}\right)^2, \tag{5}$$

where M_0 is the (temperature-dependent) equilibrium value of the magnetic moment of the bulk material, $\chi_\parallel$ is the static equilibrium value of the parallel susceptibility of the material; below the critical temperature $\chi_\parallel \ll 1$. For the longitudinal dynamics only the parallel part of the effective field, H_{eff}, enters the problem,

$$H_{\text{eff}} = -\frac{1}{2\chi_\parallel M_0^2}\left(M^2 - M_0^2\right)M + A\frac{\partial^2 M}{\partial x^2}.$$

Substituting the explicit form of the H_{eff} into Eq. (4), dividing Eq. (4) by M_0, and introducing dimensionless variables, one obtains

$$\frac{\partial m(\xi,t)}{\partial t} = \left[m_0^2(\xi) - m^2(\xi,t)\right]m(\xi,t) + \frac{\partial^2 m(\xi,t)}{\partial \xi^2} - \varepsilon \frac{\partial^2}{\partial \xi^2}\left\{\left[m_0^2(\xi) - m^2(\xi,t)\right]m(\xi,t) + \frac{\partial^2 m(\xi,t)}{\partial \xi^2}\right\}, \tag{6}$$

where the dimensionless coordinate ξ is used, the time is measured in units of t_0, which is of order of the time of uniform

relaxation of the total spin, and the quantity ε is the ratio of the nonlocal (exchange) and relativistic relaxation constants, viz.

$$\xi = \frac{x}{x_0}, \quad x_0^2 = 2A\chi_\parallel, \quad t_0 = \frac{2\chi_\parallel}{\lambda_r}, \quad \varepsilon = \frac{\lambda_{nl}}{\lambda_r}. \qquad (7)$$

The value of x_0 for temperatures far from the Curie temperature is of the order of a few lattice constants [51], but it becomes large in the vicinity of the critical temperature. It is worthwhile to note here that it is difficult to make formal arguments for the use of any kind of continuous differential equation for nonuniform states with the characteristic scale of the order of the lattice spacing. However, the comparative analysis of discrete and continuous models for magnetic vortices [61] and domain walls [62] in highly anisotropic magnets shows quite good agreement even for the characteristic sizes like 1.5–2 lattice constants, and hence, we believe that our approach gives a good approximation to the problem.

To model the Ni-Fe heterostructure we choose the interface between the metals as the $\xi = 0$ point; the region $\xi < 0$ corresponds to Ni and $\xi > 0$ to Fe. For the magnetization in the nonuniform magnets, we have chosen the parameter function $m_0(\xi)$ such that the values of m_0 are different in different layers. For the concrete calculations, the values $m_0 = 1$ inside the nickel layer and $m_0 = \pm 1.5$ inside the iron layer were chosen; the signs $(+)$ and $(-)$ correspond to the parallel configuration (PC) and antiparallel configuration (AC), respectively. Thus, the value of M is normalized to the equilibrium magnetization of nickel.

The values of the material parameters $\chi_\parallel$, A, λ_r, and λ_{nl} are different in the Ni, Ru, and Fe layers. However, as our aim is to demonstrate the general features of the problem we assume that the values of the material parameters in Eqs. (6) and (7) are the same for all layers of the system. This assumption simplifies the calculations and gives us the possibility to understand the role of the different relaxation channels.

There is in addition the interlayer magnetic (RKKY) coupling, which depends on all layers and could be ferromagnetic or antiferromagnetic, depending on electronic structure properties of the interface. The most interesting case is the weak antiferromagnetic coupling, for which the layer magnetizations of the stack (parallel or antiparallel) can be changed by a relatively weak magnetic field (in the recent experiment [25], such a case is realized by ~20 mT for a 1-nm-thick Ru layer). This relatively small quantity does not influence the magnetization relaxation. For the two alternative configurations, we will see below a large difference in the spin-dynamics behavior, despite the fact that the sign of the coupling is the same.

Within the considered model systems of contacted layers of different magnets, the interfaces are considered very thin, but of finite width, of the order of one atomic size; hence, a space-dependent $m_0^2 = m_0^2(\xi)$ should be considered. Specifically, for the Ni-Fe system the following simple functions are chosen:

$$m_0(\xi) = \tfrac{5}{4} + \tfrac{1}{4}\tanh(\xi),$$

for PC, and

$$m_0(\xi) = -\tfrac{1}{4} - \tfrac{5}{4}\tanh(\xi),$$

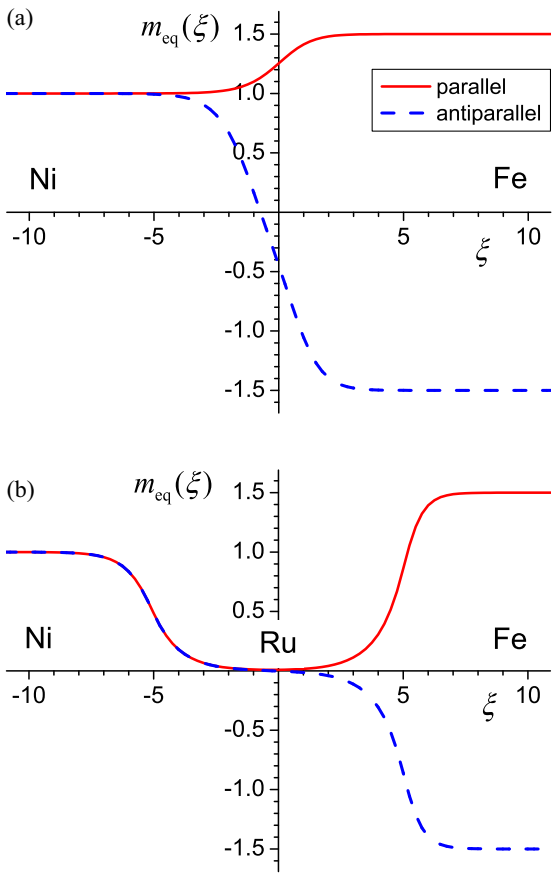

FIG. 1. (Color online) The equilibrium magnetization profile m_{eq} calculated from the solution of the equation $H_{\text{eff}} = 0$. (a) The profile of the Ni-Fe system; (b) that of the Ni-Ru-Fe system. Here and henceforth in all consecutive figures, red lines correspond to the parallel and blue lines correspond to the antiparallel magnetization configuration, respectively.

for AC. Note that near boundaries between the materials proximity effects are expected and the equilibrium distribution of the magnetization $m_{eq}(\xi)$ differs from $m_0(\xi)$. The equilibrium distribution of the magnetization can be found through the solution of the equation $H_{\text{eff}}(m_{eq}) = 0$.

For the Ni-Ru-Fe heterostructure the middle of the Ru layer is adopted as $\xi = 0$. To account for the Ru layer, we assume that inside the Ru layer the parameter $m_0^2(\xi)$ has a negative value. For this system we will keep the full thickness of Ni-Ru-Fe system as 50 dimensionless units, with the thickness of the Ru layer equal to ten dimensionless units. In Fig. 1 the calculated equilibrium magnetizations m_{eq} are plotted for the Ni-Fe and Ni-Ru-Fe systems.

Thus, the initial conditions for Eq. (6) can be cast in the form $m(\xi,0) = m_{eq}(\xi) + \Delta m(\xi)$, where for $m_{eq}(\xi)$ we use the numerical results presented in Fig. 1 and the term $\Delta m(\xi)$ is an *initial redistribution of the magnetization*. This initial distribution of the magnetization is taken to be the resulting magnetization emerging after the laser-created nonequilibrium electron distribution has thermalized. This process is known [32–34] to be completed within 300–400 fs. This magnetization distribution can, e.g., be taken as the final distribution found within the superdiffusive approach [13,31].

For the numerical solution of the PDE (6) we assume free boundary conditions (the first and the second derivatives at edges of a sample are zero). Additionally, we use a condition $\int \Delta m(\xi) d\xi = 0$, which means that the total magnetization of the system remains unchanged after the first "femtosecond" stage.

In the numerical investigations, presented below, we have considered the spin relaxation for two opposite limit cases, for $\varepsilon = 200$, where the nonlocal relaxation actually controls the situation, and for $\varepsilon = 0.1$, where the relativistic relaxation dominates. First of all, in Sec. III we will present results for the simpler Ni-Fe system, and subsequently we will account for the presence of the nonmagnetic (ruthenium) layer between the ferromagnetic metals (in Sec. IV).

III. RESULTS: THE Ni-Fe SYSTEM

We start with considering the Fe-Ni model system with a direct interface between the Fe and Ni layers, for different values of the ratio of the nonlocal (exchange) constant to the local (relativistic) damping constant, ε. We will discuss this heterostructure by considering two different spin redistributions, namely the uniform redistribution, for which some part of the magnetization is homogeneously removed from Ni, after which it is homogeneously added to the Fe magnetization, and, secondly, a dip-peak shaped redistribution.

For the concrete analysis of the uniform redistribution the condition will be chosen as

$$\Delta m(\xi) = c \tanh(\xi/2), \tag{8}$$

where the parameter c gives what part of the magnetization is removed from Ni (here and further below we omitted in the equations exponential corrections caused by the finiteness of the system size). The initial distributions are shown in Fig. 2(a).

An alternative case is that of a nonuniform "dip-peak" redistribution, in which some part of the magnetization of Ni is removed from a region, located close to an interface between the two metals, and this magnetization is added in a region of the Fe layer, again close to the interface. In fact, the latter dip-peak magnetization redistribution [see Fig. 2(b)] is consistent with the final distribution found within the superdiffusive approach [25,31].

We approximate the dip-peak distribution as

$$\Delta m(\xi) = \frac{2eA^2}{cL}\xi \exp\left(-\frac{2eA^2}{c^2L^2}\xi^2\right). \tag{9}$$

Here and henceforth, L is the full size of the system (the thickness of the single Ni or Fe layer is $L/2$ for the Ni-Fe system), c is a part of the magnetization moved from Ni to Fe, the parameter A equals to relative height of the peaks and $e \simeq 2.718\,28$ is Euler's number. Below the following values will be used for the explicit analysis of the Ni-Fe system: $c = 0.2$, as this gives a reasonable value (20%) of the removed magnetization amount, $L = 50$, as it corresponds to the thickness of the Ni and Fe layers of the order of several nanometers and $A = 0.9$. In addition, in Sec. III C some other initial states will be discussed.

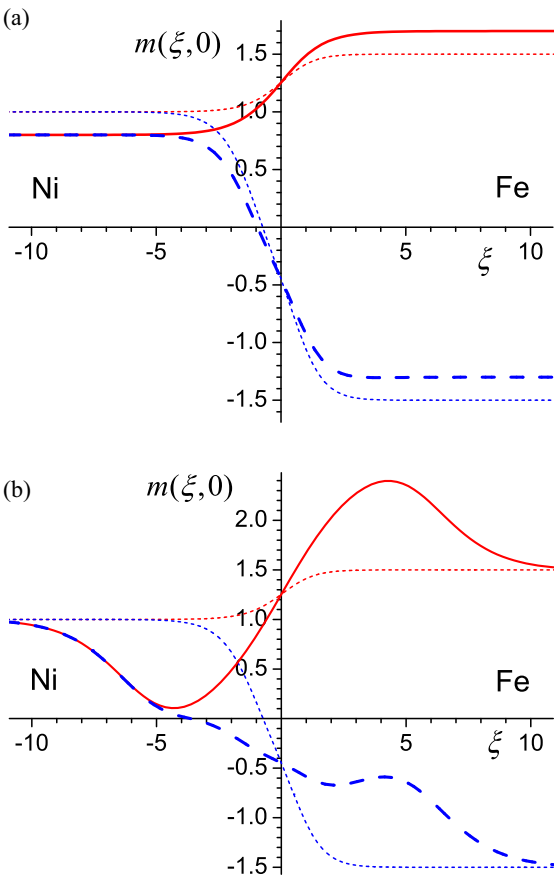

FIG. 2. (Color online) (a) Initial magnetization distributions for homogeneous magnetization displacement, $m(\xi,0) = m_{eq}(\xi) + 0.2\tanh(\xi/2)$. The thin dotted lines here and in following figures depict the equilibrium magnetization distribution $m_0(\xi)$. (b) Initial magnetization distributions $m(\xi,0) = m_{eq}(\xi) + \Delta m(\xi)$ for a dip-peak-shaped starting magnetization redistribution located near the interface.

A. Ni-Fe, uniform spin redistribution

1. *Small nonlocality, $\varepsilon = 0.1$*

Figure 2 shows the initial distributions of the magnetization for PC and AC configurations. The results calculated with Eq. (6) are plotted in Fig. 3; they demonstrate that the time evolution of magnetization in the Ni layer proceeds almost independently of that in the Fe layer.

One can easily find an approximate description of the time evolution of the magnetization starting from the quasiuniform redistribution (8). Since both the value of the equilibrium magnetization $m_0(\xi)$ and the value of $\Delta m(\xi)$ in the redistribution (8) are independent on the coordinate, except for in a small region near the boundary, one can suppose that $m_0^2(\xi) = 1$ and $\Delta m(\xi) = -c$ in the Ni layer. Under these two simplifying assumptions the magnetization dynamics is independent of the coordinate in the Ni layer and terms with spatial derivatives in Eq. (6) can be omitted. These assumptions lead immediately to the simple ordinary differential equation $\partial m/\partial t = m - m^3$. Integrating this equation and multiplying the derived $m(t)$ by the size of the Ni layer, one obtains an approximate formula for the time-dependent magnetization of the Ni

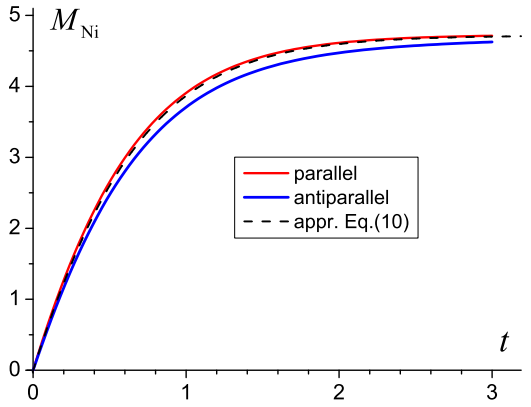

FIG. 3. (Color online) Time evolutions of the total magnetization in the Ni layer from its initial value, both for parallel and antiparallel configurations ($\varepsilon = 0.1$) The dashed line presents the approximate result from Eq. (10). Note that here and henceforth in corresponding figures the value of the function $M_{Ni}(t)$ at $t = 0$ is chosen as zero, i.e., only the essential remagnetization dynamics is shown.

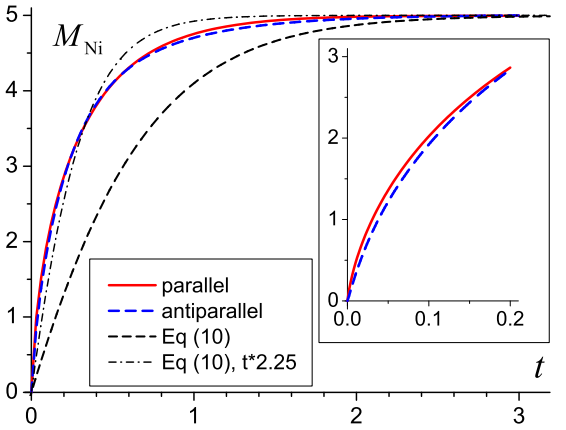

FIG. 4. (Color online) The computed magnetization evolutions of Ni for parallel and antiparallel configurations ($\varepsilon = 200$), for the case of homogeneous redistribution. For easy comparison to the calculation with $\varepsilon = 0.1$, the approximate dependence given by Eq. (10) is depicted by the dashed line. Also, some results of fitting with the scaled Eq. (10) are presented, see the text. The inset shows the remagnetization dynamics at short times.

layer,

$$M_{Ni}(t) = \frac{L(1-c)}{2\sqrt{(1-c)^2 + [1-(1-c)^2]\exp(-2t)}}. \qquad (10)$$

Figure 3 shows that there is good agreement of the analytical formula (10) with the numerical data. The small discrepancy is caused by the region close to the boundary between the metals, where both the equilibrium magnetization $m_{eq}^2(\xi)$ and the initial redistribution (8) depend on the coordinate.

In the linear approximation, $c \to 0$, Eq. (10) transforms to $M_{Ni}(t) \simeq (L/2)[1 - c\exp(-2t)]$, with the relaxation time equal to 0.5, whereas the numerical values are 0.63 for PC and 0.67 for AC. Thus, the role of the nonlinear effect, which reduces the speed of the relaxation for nonsmall m, is important. Further we will use the dependence (10) as a reference curve to compare with evolutions of the magnetization of the Ni layer, both for different redistributions and for different values of the parameter ε.

2. *Large nonlocal term,* $\varepsilon = 200$

The computed results, presented in Fig. 4, show that when assuming a large nonlocal term $\varepsilon = 200$, the recovery of the Ni magnetization becomes faster than for the case $\varepsilon = 0.1$ (for the chosen parameters roughly three times faster). The surprising fact is that the time dependence of the total magnetic moment of the Ni subsystem—as for the local case $\varepsilon = 0.1$—is practically independent on the state of the system, parallel or antiparallel. Moreover, for the considered strong nonlocal damping term the difference between the behavior for AC and PC states is even weaker than for the case $\varepsilon = 0.1$.

To understand this result and to summarize our finding for an almost uniform redistribution, we present a more detailed consideration, including the analysis of the time-resolved relaxation process, illustrated in Fig. 5.

The data presented in this figure show that the character of the evolution is completely different for all cases of interest, different configurations and (or) different ε's. The difference in the local and nonlocal dissipation scenarios manifests itself in the fact that the time dependence of M_{Ni} cannot be fitted by rescaling the time (like $t \to \eta t$, with η a fitting parameter) in the simple formula (10); compare Figs. 3 and 4. As expected, see above, for the case $\varepsilon = 0.1$, the spin relaxation becomes almost local at different points of the sample; see the dashed lines in Figs. 5(a) and 5(b). In contrast, for the case $\varepsilon = 200$ the formation of a front of the longitudinal spin relaxation takes place; one can recognize a "spin flow" from right to left in both Figs. 5(a) and 5(b). The region where this flow is seen is appreciably wide, exceeding the width of the interface region.

The shapes of the functions $m(\xi,t)$ are different for PC and AC. The behavior of the *difference* of the instantaneous magnetization and its equilibrium value is however much more similar for these two states, especially in the Ni region, see Fig. 5(c), despite the difference in some local details, e.g., the presence of the "hump" near the interface for AC. These humps are local accumulations of spin and they are likely associated with those points, where the effective field—which is a driving force for the spin current—is small; see Fig. 5(d). Thus, the similarity of the integrated characteristics in M_{Ni} can be present even for processes with different spatial-temporal behavior. As we will see below, for other sorts of initial conditions, not only the details of instantaneous distributions, but also the integral characteristics like the time-dependence of $M_{Ni}(t)$ are dissimilar for the two alternative configurations of the system, PC and AC.

B. Dip-peak-shaped spin redistribution

Next we consider a different initial spin distribution, namely, the highly nonuniform redistribution having the bipolar form of a minimum and a maximum; see Eq. (9). Such bipolar shaped redistribution is more realistic from the concept of superdiffusive spin quenching [27,31]. Note that such a bipolar shaped spin redistribution gives completely different shapes for the initial distributions of the layer magnetizations in the cases of PC and AC; see Fig. 2(b).

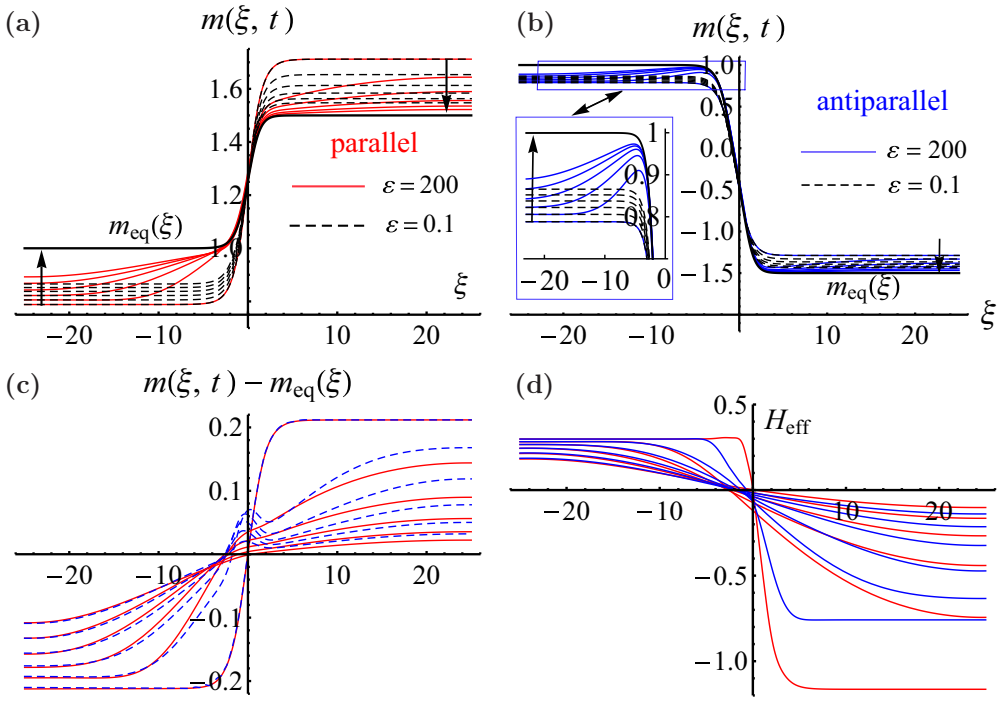

FIG. 5. (Color online) Time evolutions of the layer-resolved magnetization $m(\xi,t)$ for the homogeneous initial conditions $m(\xi,0) = 0.2\tanh\xi$, shown for successive times computed with a time step $\Delta t = 0.06$, for parallel (a) and antiparallel (b) configurations, respectively. Results obtained for different values of ε are shown. The data for a dominating nonlocal dissipation ($\varepsilon = 200$) are present by full lines, red and blue colors give PC and AC, respectively. The data obtained for $\varepsilon = 0.1$ are depicted by black dashed lines in both panels. The inset to panel (b) presents the data on a different scale, comparable to that in panel (a). Vertical arrows indicate the directions of time evolution. Panel (c) presents the time evolution of the deviation of the magnetization from the equilibrium and panel (d) shows the time evolution of the effective field H_{eff}, for $\varepsilon = 200$.

1. *Small nonlocal term,* $\varepsilon = 0.1$

The computed evolutions of the Ni magnetization for both PC and AC are presented in Fig. 6. Curiously, in spite of the locality of the dominating relativistic damping term, the time evolution of Ni strongly depends on the orientation of the Fe magnetization. Such behavior of a spin system—for an initial spin redistribution located near a boundary—is a consequence of the following effects: (i) even for $\lambda_{nl} = 0$, diffusive effects caused by the term $A\nabla^2 M$ are present in the LLBar equation. (ii) the state of Fe changes the equilibrium magnetization of Ni in a region of the order of a few atomic sizes, and, as it follows from Eq. (6), influences the recovery speed of Ni (close to the interface). We also would like to emphasize that for a spin redistribution comparable to that obtained within the superdiffusive approach, our relaxation data can no longer be fitted by an exponential function.

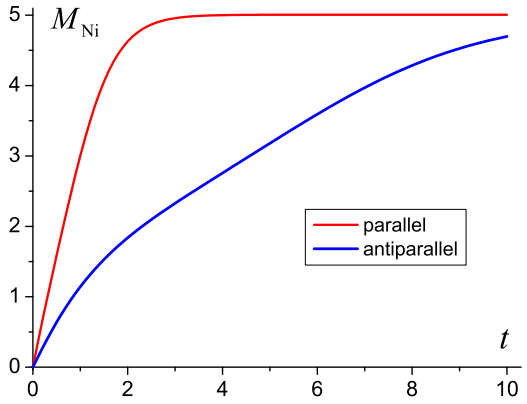

FIG. 6. (Color online) Calculated time evolutions of the total magnetization of the Ni layer for parallel and antiparallel configurations ($\varepsilon = 0.1$) for a starting dip-peak spin redistribution localized at the interface.

2. *Large nonlocal term,* $\varepsilon = 200$

Considering next the case of large nonlocal effects, we find that the spin recovery of the Ni layer for a bipolar spin redistribution proceeds much faster for $\varepsilon = 200$ than for $\varepsilon = 0.1$ (for the here-used parameters roughly 50 times). In addition, the results given in Fig. 7 show that the Ni spin relaxation does depend substantially on the alignment of the Fe spin to that of the Ni spin. However, we find, for this system and under these conditions, that the PC still exhibits faster spin relaxation, whereas the recent experiments showed an opposite behavior [25].

The recovery behavior for $\varepsilon = 200$ is fully determined by the nonlocal damping features which strongly relate to the difference in the initial distributions for AC and PC states. As one can see from the data given in Fig. 2 (bottom), well-defined peaks of different signs are present for PC, whereas for AC such peaks are "absorbed" by the nonuniformity of the interface. The initial stage of the dissipation process for

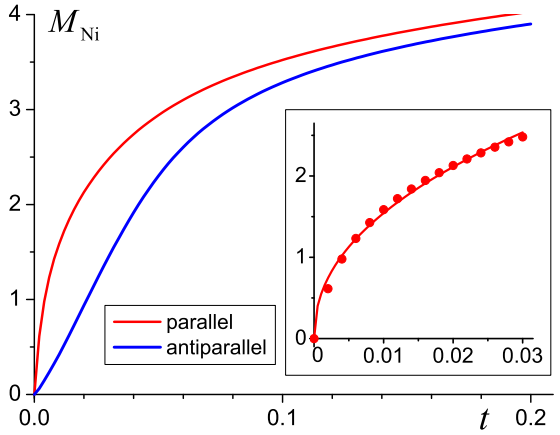

FIG. 7. (Color online) Time evolutions of the Ni magnetization for parallel and antiparallel Ni-Fe configurations, computed for the localized bipolar initial spin redistribution and $\varepsilon = 200$. In the inset the initial stage of the PC relaxation is presented together with the fit by a square-root dependence.

PC can qualitatively be treated as a spin diffusive widening of both peaks, with the "annihilation" of the magnetization of one peak through moving to the region of the magnetization dip; see Fig. 8. This scenario is confirmed by the nearly square-root dependence of $M_{\mathrm{Ni}}(t)$ taking place for PC; see the inset of Fig. 7. Conversely, the time dependence of the magnetization is almost linear for AC. Probably, such a diffusive scenario, caused by the contribution from nonuniform exchange to the effective field, is responsible for the observed difference of the relaxation rates for AC and PC, even for the model with $\varepsilon = 0.1$; see Fig. 6.

To summarize our findings, for all above-considered cases the general observation is the following: the spin relaxation in Ni occurs faster for the PC than for the AC. This is in contradiction with the experimental observation, which shows that the recovery of the total magnetic moment of nickel occurs faster for the AC state of the system [25].

C. Dip-peak-shaped spin redistributions with different peak positions and widths

The conclusion from the above simulations is that, in order to find the regimes with faster relaxation for AC, we need to consider some differently shaped initial spin distributions. In the above calculations we have used the same $\Delta m(\xi)$ for both PC and for AC. The data found within the superdiffusive approach could be a good guide for seeking appropriate distributions. In the superdiffusive data the final nonequilibrium spin redistribution for AC looks a little bit sharper than for PC [25,31]. Hence, we will assume next a sharper redistribution for AC. In advance to showing the results, we mention that we have found that such initial states, for the model with nonsmall nonlocal relaxation term, could lead to the desired result, i.e., provide agreement with the experiment.

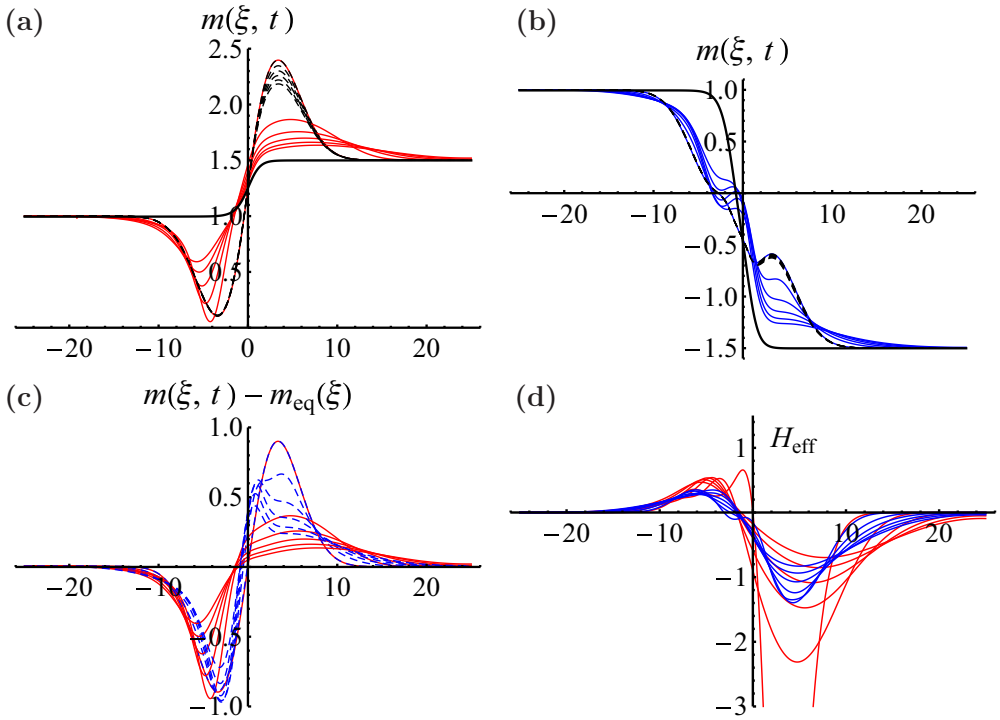

FIG. 8. (Color online) Time evolutions of the magnetization $m(\xi,t)$ computed for the localized dip-peak initial spin redistribution, shown for successive times computed at time steps $\Delta t = 0.06$, for parallel (a) and antiparallel (b) configurations, respectively. Results are shown for different values of ε. The data for a dominating nonlocal dissipation ($\varepsilon = 200$) are present by full lines, red and blue lines give PC and AC, respectively. The data for small nonlocal spin dissipation ($\varepsilon = 0.1$) are depicted by black dashed lines in panels (a) and (b). Panels (c) and (d) present the time evolution of the deviation of the magnetization from the equilibrium and the time evolution of the effective field H_{eff}, respectively, for $\varepsilon = 200$.

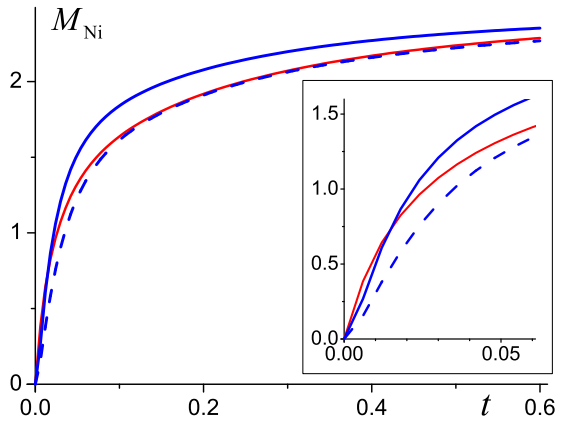

FIG. 9. (Color online) Time evolutions of the Ni magnetization for parallel and antiparallel magnetization configurations, calculated for the localized initial spin redistribution and $\varepsilon = 200$. Using the same redistribution $\Delta m(\xi)$ for both PC and AC, a slightly faster spin relaxation occurs for PC (red line) than for AC (dashed blue line). However, AC recovers faster than PC when a sharper spin redistribution for AC than for PC has been used (except for extremely short times; see inset).

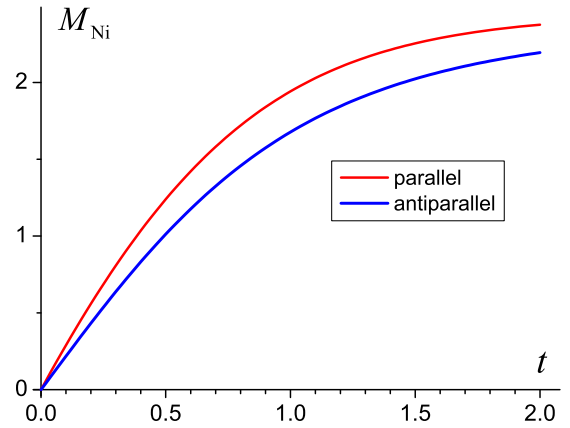

FIG. 10. (Color online) Time evolutions of the Ni layer magnetization for the same initial spin redistributions as adopted in Fig. 9 (with a sharper peak for AC) but employing a dominant relativistic damping $\varepsilon = 0.1$.

We consider some different initial redistributions having a bipolar shape, where the dip and peak are placed deep inside the Ni and Fe layer, respectively. These spin redistributions can be modeled by the function

$$\Delta m(\xi) = -A_{\mathrm{Ni}} \exp\left[-\pi\left(\frac{2A_{\mathrm{Ni}}}{cL}\right)^2 (\xi + \xi_{\mathrm{Ni}})^2\right] + A_{\mathrm{Fe}} \exp\left[-\pi\left(\frac{2A_{\mathrm{Fe}}}{cL}\right)^2 (\xi - \xi_{\mathrm{Fe}})^2\right], \quad (11)$$

where ξ_{Fe} and ξ_{Ni} stand for the distances of the peaks in the Fe and Ni layers, measured from the boundary between the metals, and the parameters A_{Ni} and A_{Fe} are the amplitudes of the peaks in the Ni and Fe layers. For the concrete analysis of these dip-peak-shaped redistributions the part of the magnetization moved from Ni to Fe is chosen as $c = 0.1$.

The results of the analysis of the evolution of the total Ni spin for equivalent peaks in both AC and PC ($A_{\mathrm{Ni}} = A_{\mathrm{Fe}} = 0.45$ and $\xi_{\mathrm{Fe}} = \xi_{\mathrm{Ni}} = 5$) are shown in Fig. 9. As was the case for the previous considerations, PC relaxes slightly faster for this initial distribution. In a next step, we use peak-shaped initial conditions of the form of Eq. (11), yet with a sharper peak in the Fe layer for AC. Specifically, the peak in the Fe layer is chosen to be higher, and hence narrower, and is situated closer to the interface, with the concrete values $A_{\mathrm{Ni}} = 0.6$, $A_{\mathrm{Fe}} = 0.9$, and $\xi_{\mathrm{Ni}} = 4$, $\xi_{\mathrm{Fe}} = 2.5$. In fact, doing so we try to model the form of Δm found within the superdiffusive approach [31].

The results presented in Fig. 9 evidence that for this modification of the bipolar distribution the magnetization recovery in the AC becomes faster. This implies that such distributions provide a way to explain the experiment. Note that this faster relaxation for AC, shown in Fig. 9, appears because of two assumptions: the sharper peak of the initial spin redistribution in the Fe region in the case of AC and the dominant role of the nonlocal spin relaxation (large ε). The time evolution of the Ni magnetization for the same initial conditions as used in Fig. 9, but for dominating relativistic damping ($\varepsilon = 0.1$), is presented in Fig. 10. One recognizes that in spite of using a sharper spin redistribution for AC, the PC relaxation is again faster than that of AC. This is one more evidence of the fact that the time evolution of the Ni magnetization in the Ni-Fe bilayer system crucially depends on the parameter ε.

The derived conclusions should however not depend on particularities of an assumed initial spin redistribution. We have therefore repeated the analysis for some other types of initial magnetization redistributions, with different peak shapes and (or) bipolar functions. All these calculations did show that in the case of a dominating relativistic spin relaxation, the relaxation of the PC is always faster than that of AC (the red lines, corresponding to PC, are always above the blue lines of AC in the figures). For a dominating nonlocal relaxation term ($\varepsilon = 200$) the situation is more diverse; for some special kinds of initial spin redistributions the relaxation for AC becomes a little bit faster than for PC. Thus, our simulations demonstrate the principal possibility to control the speed of spin relaxation in coupled bilayers by manipulating the initial spin redistributions.

For $\varepsilon = 0.1$ the local recovery process of the Ni magnetization depends on the value of the Fe magnetization, especially for initial redistributions localized near the interface between the metals. But for all used redistributions PC exhibits a faster spin relaxation than AC. Thus, in spite of the richness of physical processes in nanometer size systems for $\varepsilon = 0.1$, for our purpose relativistic relaxation appears uninteresting as under such circumstance PC is always faster than AC (while in the experiment [25] an opposite situation was observed).

Conversely, for $\varepsilon = 200$, we have demonstrated, by using sharper spin redistributions for AC (comparable to the final redistributions appearing after completing the initial nonequilibrium stage) that the spin relaxation of the AC can be faster than for PC (around 20%).

IV. RESULTS: THE Ni-Ru-Fe SYSTEM

As illustrated in Fig. 1(b), the presence of the Ru-spacer layer makes the transition in the equilibrium magnetization profile from Ni to Fe for PC sharper than for the simpler Ni-Fe system. For AC an opposite scenario is realized; here, $m(\xi,0)$ seems to be smoother. This difference offers an additional opportunity for achieving better agreement with the experiment. In the previous analysis we have found that the high rate of the nonlocal spin relaxation is necessary for explaining the experiment. In addition, the influence of the nonlocal relaxation term is found to be more pronounced for a sharp initial distribution $m(\xi,0) = m_{eq}(\xi) + \Delta m(\xi)$. In the Ni-Fe system the transition from Ni to Fe and the initial redistributions $\Delta m(\xi)$ enhance each other so that the resulting distribution $m(\xi,0)$ becomes more inhomogeneous. Therefore, the variation of the magnetization from Ni to Fe in the Ni-Fe system enhances the relaxation of PC. As mentioned, the presence of the Ru layer could be expected to reduce this enhancement.

To verify this hypothesis we analyze the following explicit examples. We consider the model for the Ni-Ru-Fe system, with a total thickness of the size of 50 dimensionless units, of which the Ru-layer thickness equals ten dimensionless units. To investigate the spin relaxation process, we solve Eq. (6), where the presence of Ru layer is accounted for by setting the parameter $m_0^2(\xi) = -1$ inside the Ru layer; see Sec. II A above. The calculated equilibrium magnetization profile $m_{eq}(\xi)$ for the Ni-Ru-Fe system is shown in Fig. 1(b) above.

The initial conditions we again represent by the form $m(\xi,0) = m_{eq}(\xi) + \Delta m(\xi)$. It is worth noting that the presence of the Ru layer was not taken into account in the simulations within the superdiffusive approach [25]. Consequently, we have no firm picture of how the initial nonequilibrium magnetization peaks are positioned in the layers with respect to the boundaries between the metals. Again, we need to try different initial nonequilibrium states in the analysis of the macroscopic spin-density evolution.

To approximate the shape of the laser-induced spin redistribution $\Delta m(\xi)$ in the Ni-Ru-Fe trilayer system we also use Eq. (11), but the parameters have the following values: $L = 50$ is the size of the system (thicknesses of Ni, Ru, and Fe layers are 20, 10, and 20, respectively), ξ_{Ni} and ξ_{Fe} are the positions of peaks relative to the middle of the Ru layer ($\xi = 0$), and $c = 0.1$ is the part of the magnetization removed from Ni. To start with, we calculate the spin relaxation for both PC and AC using the same initial redistribution, consisting of two equivalent peaks, as in Eq. (11) above, with the values $\xi_{\mathrm{Ni}} = 6$ and $\xi_{\mathrm{Fe}} = 4$. For such $\Delta m(\xi)$, 10% of the total magnetic moment is redistributed. We consider first the process for the initial conditions with equivalent peaks both for PC and for AC. The results given in Fig. 11 demonstrate that the spin-relaxation processes of Ni will be almost equivalent for PC and AC. Next, following the previous results, we construct a sharper peak for AC, with $A_{\mathrm{Ni}} = 0.6$ and $A_{\mathrm{Fe}} = 0.9$, and with $\xi_{\mathrm{Ni}} = 4$ and $\xi_{\mathrm{Fe}} = 2.5$, with the same value of the magnetization removed from Ni layer, $c = 0.1$. From the computed results shown in Fig. 11 one can see that for this case the recovery of the Ni magnetization is around two times faster for AC than for PC.

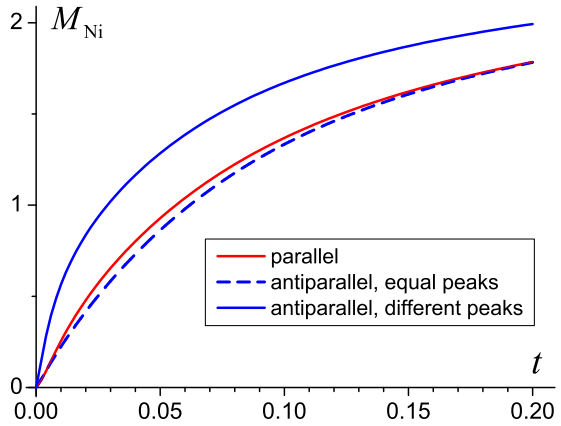

FIG. 11. (Color online) Time evolutions of the Ni magnetization for parallel and antiparallel magnetization configurations in the Ni-Ru-Fe system, computed for the localized initial spin redistribution and $\varepsilon = 200$. Adopting the same spin redistribution $\Delta m(\xi)$ both for PC and AC a similar relaxation behavior is obtained for PC (red line) and AC (dashed blue line). The Ni magnetization recovers faster for AC than for PC if a sharper initial redistribution for AC than for PC has been adopted (blue line).

Again, as for the Ni-Fe system, the experimentally obtained behavior, namely, the faster relaxation for AC, appears only for the system when the nonlocal damping dominates. For the same initial conditions with two nonequivalent peaks, but for the same trilayer model with $\varepsilon = 0.1$, the spin-relaxation times for AC and PC configurations become practically equivalent (yet with an even smaller difference between red PC and blue AC curves as present in Fig. 3 above; not shown here). This observation once more confirms our conjecture of the importance of the nonlocal (exchange) relaxation.

V. CONCLUSIONS

We have developed a theoretical formulation to describe the longitudinal, fast spin dynamics in coupled magnetic layers. Several starting nonequilibrium spin distributions have been considered in the calculation of the consecutive occurring spin evolution. Our calculations demonstrate the principal possibility of controlling the relaxation processes in nanometer-size layered systems both in the case of purely relativistic and of nonlocal magnetization dampings. For example, by selecting special forms of the initial redistributions, the spin relaxation of the antiparallel configuration can be made faster than that of the parallel configuration, as has been detected in the recent experiments on metallic trilayers [25,26]. This we find to be the case both for the simple Ni-Fe and more complicated Ni-Ru-Fe heterostructures, for the identified initial spin conditions.

In addition to the discussed layer-resolved measurements on metallic trilayers, we note that faster magnetization recovery dynamics has recently been observed, too, for the antiparallel state of magnetic tunnel junctions consisting of two CoFeB layers separated by a thin MgO barrier [28].

The magnetization recovery is also found to be sensitive to the presence of the nonmagnetic Ru layer. Namely, for the Ni-Ru-Fe trilayer we have obtained that in the AC the spin recovery occurs almost two times faster than in the PC. Thus, our approach provides an opportunity for the qualitative

description of the experiment. Especially, this steering of the magnetization evolution is found to be efficient for materials with strong nonlocal damping (large ε). Additionally, for large ε we obtain a clear manifestation of spin flow instead of local relaxation, i.e., a spin current resulting from the initial nonequilibrium state in conjunction with the nonlocal relaxation. This spin current is clearly seen as a flow of spin in the heterostructures for different initial spin distributions; see Figs. 5 and 8. Our analysis underlines that such fast spin currents can typically be anticipated in heterostructures with strongly nonequilibrium spin distributions.

To conclude, our theory predicts the important effect of the fast nonlocal evolution of the longitudinal magnetization of magnetic layered systems (synthetic ferrimagnets), which is very sensitive to the details of the initial spin redistributions. A future dream could of course be to construct something like an "inverse method," which gives the possibility to predict some details of the initial spin redistribution through the analysis of integral characteristics, like time dependencies of the magnetic moment of some specific layer or so. At present the equations are however too complicated for realization of such a theory. Conversely, designing specific starting spin conditions could pave a way to achieving an exceptionally fast remagnetization. As we have shown, the presence/absence of peaks in the initial spin redistribution and even the presence/absence of differences in the widths of the peaks leads to clearly detected effects for these characteristics. In particular, the possibility of having a faster spin recovery for the antiparallel configuration of a system is observed, and the conditions under which these occur have been established here. Fast longitudinal spin dynamics under such conditions would provide an explanation of the recent experimental observations [25,26,35].

ACKNOWLEDGMENTS

We thank V. G. Bar'yakhtar, M. Battiato, K. Carva, and P. Maldonado for helpful discussions. This work has been supported by the Swedish Research Council (VR) and the European Community's Seventh Framework Programme (FP7/2007-2013) under Grant Agreement No. 281043, FemtoSpin. The work in Kiev has been partly supported by the Government of Ukraine, state program "Nanotechnologies and Nanomaterials" and by the State Foundation of Fundamental Research of the Ukraine via Grant No. F53.2/045.

[1] E. Beaurepaire, J.-C. Merle, A. Daunois, and J.-Y. Bigot, Phys. Rev. Lett. **76**, 4250 (1996).
[2] B. Koopmans, M. van Kampen, J. T. Kohlhepp, and W. J. M. de Jonge, Phys. Rev. Lett. **85**, 844 (2000).
[3] D. Cheskis, A. Porat, L. Szapiro, O. Potashnik, and S. Bar-Ad, Phys. Rev. B **72**, 014437 (2005).
[4] C. Stamm, T. Kachel, N. Pontius, R. Mitzner, T. Quast, K. Holldack, S. Khan, C. Lupulescu, E. F. Aziz, M. Wietstruk, H. A. Dürr, and W. Eberhardt, Nat. Mater. **6**, 740 (2007).
[5] A. Kirilyuk, A. V. Kimel, and Th. Rasing, Rev. Mod. Phys. **82**, 2731 (2010).
[6] G. P. Zhang and W. Hübner, Phys. Rev. Lett. **85**, 3025 (2000).
[7] B. Koopmans, J. J. M. Ruigrok, F. Dalla Longa, and W. J. M. de Jonge, Phys. Rev. Lett. **95**, 267207 (2005).
[8] E. Carpene, E. Mancini, C. Dallera, M. Brenna, E. Puppin, and S. De Silvestri, Phys. Rev. B **78**, 174422 (2008).
[9] B. Koopmans, G. Malinowski, F. Dalla Longa, D. Steiauf, M. Fähnle, T. Roth, M. Cinchetti, and M. Aeschlimann, Nat. Mater. **9**, 259 (2010).
[10] M. Krauss, T. Roth, S. Alebrand, D. Steil, M. Cinchetti, M. Aeschlimann, and H. C. Schneider, Phys. Rev. B **80**, 180407(R) (2009).
[11] G. P. Zhang, W. Hübner, G. Lefkidis, Y. Bai, and T. F. George, Nat. Phys. **5**, 499 (2009).
[12] J.-Y. Bigot, M. Vomir, and E. Beaurepaire, Nat. Phys. **5**, 515 (2009).
[13] M. Battiato, K. Carva, and P. M. Oppeneer, Phys. Rev. Lett. **105**, 027203 (2010).
[14] K. Carva, M. Battiatio, and P. M. Oppeneer, Nat. Phys. **7**, 665 (2011).
[15] K. Carva, M. Battiato, and P. M. Oppeneer, Phys. Rev. Lett. **107**, 207201 (2011).
[16] I. Radu, K. Vahaplar, C. Stamm, T. Kachel, N. Pontius, H. A. Dürr, T. A. Ostler, J. Barker, R. F. L. Evans, R. W. Chantrell, A. Tsukamoto, A. Itoh, A. Kirilyuk, Th. Rasing, and A. V. Kimel, Nature (London) **472**, 205 (2011).
[17] S. Mathias, C. La-O-Vorakiat, P. Grychtol, P. Granitzka, E. Turgut, J. M. Shaw, R. Adam, H. T. Nembach, M. Siemens, S. Eich, C. M. Schneider, T. Silva, M. Aeschlimann, M. M. Murnane, and H. Kapteyn, Proc. Natl. Acad. Sci. USA **109**, 4792 (2012).
[18] B. Pfau, S. Schaffert, L. Müller, C. Gutt, A. Al-Shemmary, F. Büttner, R. Delaunay, S. Düsterer, S. Flewett, R. Frömter, J. Geilhufe, E. Guehrs, C. M. Günther, R. Hawaldar, M. Hille, N. Jaouen, A. Kobs, K. Li, J. Mohanty, H. Redlin, W. F. Schlotter, D. Stickler, R. Treusch, B. Vodungbo, M. Kläui, H. P. Oepen, J. Lüning, G. Grübel, and S. Eisebitt, Nat. Commun. **3**, 1100 (2012).
[19] B. Vodungbo, J. Gautier, G. Lambert, A. Barszczak Sardinha, M. Lozano, S. Sebban, M. Ducousso, W. Boutu, K. Li, B. Tudu, M. Tortarolo, R. Hawaldar, R. Delaunay, V. Lopez-Flores, J. Arabski, C. Boeglin, H. Merdji, P. Zeitoun, and J. Lüning, Nat. Commun. **3**, 999 (2012).
[20] C. E. Graves, A. H. Reid, T. Wang, B. Wu, S. de Jong, K. Vahaplar, I. Radu, D. P. Bernstein, M. Messerschmidt, L. Müller, R. Coffee, M. Bionta, S. W. Epp, R. Hartmann, N. Kimmel, G. Hauser, A. Hartmann, P. Holl, H. Gorke, J. H. Mentink, A. Tsukamoto, A. Fognini, J. J. Turner, W. F. Schlotter, D. Rolles, H. Soltau, L. Strüder, Y. Acremann, A. V. Kimel, A. Kirilyuk, Th. Rasing, J. Stöhr, A. O. Scherz, and H. A. Dürr, Nat. Mater. **12**, 293 (2013).
[21] N. Bergeard, V. López-Flores, V. Halté, M. Hehn, C. Stamm, N. Pontius, E. Beaurepaire, and C. Boeglin, Nat. Commun. **5**, 3466 (2014).
[22] T. A. Ostler, J. Barker, R. F. L. Evans, R. W. Chantrell, U. Atxitia, O. Chubykalo-Fesenko, S. El Moussaoui, L. Le Guyader, E. Mengotti, L. J. Heyderman, F. Nolting, A. Tsukamoto, A. Itoh, D. Afanasiev, B. A. Ivanov, A. M. Kalashnikova, K.

Vahaplar, J. Mentink, A. Kirilyuk, Th. Rasing, and A. V. Kimel, Nat. Commun. **3**, 666 (2012).
[23] J. H. Mentink, J. Hellsvik, D. V. Afanasiev, B. A. Ivanov, A. Kirilyuk, A. V. Kimel, O. Eriksson, M. I. Katsnelson, and Th. Rasing, Phys. Rev. Lett. **108**, 057202 (2012).
[24] S. Wienholdt, D. Hinzke, K. Carva, P. M. Oppeneer, and U. Nowak, Phys. Rev. B **88**, 020406(R) (2013).
[25] D. Rudolf, C. La-O-Vorakiat, M. Battiato, R. Adam, J. M. Shaw, E. Turgut, P. Maldonado, S. Mathias, P. Grychtol, H. T. Nembach, T. J. Silva, M. Aeschlimann, H. C. Kapteyn, M. M. Murnane, C. M. Schneider, and P. M. Oppeneer, Nat. Commun. **3**, 1037 (2012).
[26] E. Turgut, C. La-o-vorakiat, J. M. Shaw, P. Grychtol, H. T. Nembach, D. Rudolf, R. Adam, M. Aeschlimann, C. M. Schneider, T. J. Silva, M. M. Murnane, H. C. Kapteyn, and S. Mathias, Phys. Rev. Lett. **110**, 197201 (2013).
[27] A. Eschenlohr, M. Battiato, P. Maldonado, N. Pontius, T. Kachel, K. Holldack, R. Mitzner, A. Föhlisch, P. M. Oppeneer, and C. Stamm, Nat. Mater. **12**, 332 (2013).
[28] W. He, T. Zhu, X.-Q. Zhang, H.-T. Yang, and Z.-H. Cheng, Sci. Rep. **3**, 2883 (2013).
[29] S. Mangin, M. Gottwald, C.-H. Lambert, D. Steil, V. Uhlir, L. Pang, M. Hehn, S. Alebrand, M. Cinchetti, G. Malinowski, Y. Fainman, M. Aeschlimann, and E. E. Fullerton, Nat. Mater. **13**, 286 (2014).
[30] R. F. L. Evans, T. A. Ostler, R. W. Chantrell, I. Radu, and Th. Rasing, Appl. Phys. Lett. **104**, 082410 (2014).
[31] M. Battiato, K. Carva, and P. M. Oppeneer, Phys. Rev. B **86**, 024404 (2012).
[32] C. Guo, G. Rodriguez, and A. J. Taylor, Phys. Rev. Lett. **86**, 1638 (2001).
[33] H.-S. Rhie, H. A. Dürr, and W. Eberhardt, Phys. Rev. Lett. **90**, 247201 (2003).
[34] M. Lisowski, P. A. Loukakos, U. Bovensiepen, J. Stähler, C. Gahl, and M. Wolf, Appl. Phys. A **78**, 165 (2004).
[35] D. Rudolf, Ph.D. thesis, Forschungszentrum Jülich, Germany, 2013.
[36] L. D. Landau and E. M. Lifshitz, in *The Collection of Works*, edited by L. D. Landau (Nauka, Moscow 1969) [in Russian], Vol. 1, p. 128.
[37] D. A. Garanin, Phys. Rev. B **55**, 3050 (1997).
[38] V. G. Bar'yakhtar, Sov. Phys. JETP **60**, 863 (1984) [Zh. Eksp. Theor. Fiz. **87**, 1501 (1984)].
[39] V. G. Bar'yakhtar, Sov. Phys. Solid State **29**, 754 (1987) [Fiz. Tverd. Tela **29**, 1317 (1987)].
[40] V. G. Bar'yakhtar, Physica B **159**, 20 (1989).
[41] M. Dvornik, A. Vansteenkiste, and B. Van Waeyenberge, Phys. Rev. B **88**, 054427 (2013).
[42] T. L. Gilbert, IEEE Trans. Mag. **40**, 3443 (2004).
[43] F. J. Dyson, Phys. Rev. **102**, 1230 (1956).
[44] L. D. Landau and I. M. Khalatnikov, Dokl. Akad. Nauk SSSR **96**, 469 (1954); see also L. D. Landau and I. M. Khalatnikov, in *The Collection of Works* (Ref. [36]), Vol. 2, p. 218.
[45] A. I. Akhiezer, V. G. Bar'yakhtar, and S. V. Peletminskii, *Spin Waves* (North-Holland, Amsterdam, 1968).
[46] D. A. Garanin and O. Chubykalo-Fesenko, Phys. Rev. B **70**, 212409 (2004).
[47] R. F. L. Evans, D. Hinzke, U. Atxitia, U. Nowak, R. W. Chantrell, and O. Chubykalo-Fesenko, Phys. Rev. B **85**, 014433 (2012).
[48] Y. Tserkovnyak, E. M. Hankiewicz, and G. Vignale, Phys. Rev. B **79**, 094415 (2009).
[49] V. G. Bar'yakhtar, B. A. Ivanov, and K. A. Safaryan, Solid State Commun. **72**, 1117 (1989).
[50] V. G. Bar'yakhtar, B. A. Ivanov, T. K. Soboleva, and A. L. Sukstanskii, Zh. Eksp. Theor. Fiz. **91**, 1454 (1986) [Sov. Phys. JETP **64**, 857 (1986)].
[51] E. G. Galkina, B. A. Ivanov, and V. A. Stephanovich, J. Magn. Magn. Mater. **118**, 373 (1993).
[52] Note that for two-sublattice ferrimagnets with sublattice spins $\vec{S}_1$ and $\vec{S}_1$ the situation can be more complicated. For such magnets, the dynamics of the vector $\vec{L} = \vec{S}_1 - \vec{S}_1$ (corresponding to so-called optical magnons) can be as fast as the exchange times, which could lead to the coupling of longitudinal and transversal spin dynamics within exchange times; see recent articles [53,54].
[53] U. Atxitia, T. Ostler, J. Barker, R. F. L. Evans, R. W. Chantrell, and O. Chubykalo-Fesenko, Phys. Rev. B **87**, 224417 (2013).
[54] V. G. Bar'yakhtar, V. I. Butrim, and B. A. Ivanov, JETP Lett. **98**, 289 (2013).
[55] A. Kolmogorov, I. Petrovsky, and N. Piskounov, in *Dynamics of Curved Fronts*, edited by P. Pelcé (Academic, San Diego, 1988) [translated from Bulletin de l'Université d'État à Moscou, Ser. Int., Sec. A, Vol. 1, 1937].
[56] R. Fischer, Ann. Eugenics **7**, 355 (1937).
[57] V. M. Eleonskii, N. N. Kirova, and N. E. Kulagin, Zh. Eksp. Teor. Fiz. **79**, 321 (1980) [Sov. Phys. JETP **52**, 162 (1980)].
[58] I. A. Yastremsky, Fiz. Tverd. Tela **56**, 1076 (2014) [Phys. Solid State **56**, 1118 (2014)].
[59] U. Ebert and W. van Saarloos, Physica D **146**, 1 (2000).
[60] P. Collet and J. P. Eckmann, *Instabilities and Fronts in Extended Systems* (Princeton University Press, Princeton, NJ, 1990).
[61] B. A. Ivanov, A. K. Kolezhuk, and G. M. Wysin, Phys. Rev. Lett. **76**, 511 (1996).
[62] B. A. Ivanov and H.-J. Mikeska, Phys. Rev. B **70**, 174409 (2004).